Erasable superconductivity in topological insulator Bi2Se3 induced by voltage pulse

Tian Le (tianlephy@iphy.ac.cn)
Zhejiang University https://orcid.org/0000-0001-8659-1873
Qikai Ye
Zhejiang University
Chufan Chen
Zhejiang University
Lichang Yin
Zhejiang University
Dongting Zhang
Zhejiang University
Xiaozhi Wang
Zhejiang University
Xin Lu
Zhejiang University https://orcid.org/0000-0002-8156-1680

Article

Keywords: Three-dimensional topological insulators (TIs), erasable superconductivity, voltage pulse

Posted Date: November 3rd, 2020

DOI: https://doi.org/10.21203/rs.3.rs-97123/v1

Erasable superconductivity in topological insulator Bi_2Se_3 induced by voltage pulse

Tian Le * †[1], Qikai Ye[2], Chufan Chen[1], Lichang Yin[1], Dongting Zhang[1], Xiaozhi Wang ‡[2], and Xin Lu §[1,3,4]

[1] *Center for Correlated Matter and Department of Physics, Zhejiang University, Hangzhou 310058, China*

[2] *Key Labaratory of Advanced Micro/Nano Electronic Devices and Smart Systems of Zhejiang, College of Information Science and Electronic Engineering, Zhejiang University, Hangzhou 310027, China*

[3] *Zhejiang Province Key Laboratory of Quantum Technology and Device, Zhejiang University, Hangzhou 310027, China*

[4] *Collaborative Innovation Center of Advanced Microstructures, Nanjing University, Nanjing, 210093, China*

Three-dimensional topological insulators (TIs) attract much attention due to its topologically protected Dirac surface states [1, 2, 3, 4]. Doping into TIs or their proximity with normal superconductors can promote the realization of topological superconductivity (SC) and Majorana fermions with potential applications in quantum computations [5, 6, 7, 8, 9, 10, 11]. Here, we observed an emergent superconductivity in local mesoscopic point-contacts on the topological insulator Bi_2Se_3 by applying a voltage pulse through the contacts, evidenced by the Andreev reflection peak in the point-contact spectra and a visible resistance drop in the four-probe electrical resistance measurements. More intriguingly, the superconductivity can be erased with thermal cycles by warming up to high temperatures (300 K) and induced again by the voltage pulse at the base temperature (1.9 K), suggesting a significance for designing new types of quantum devices. Nematic behaviour

*Corresponding author: tianlephy@iphy.ac.cn

†Current address: Beijing National Laboratory for Condensed Matter Physics, Institute of Physics, Chinese Academy of Sciences, Beijing 100190, China

‡Corresponding author: xw224@zju.edu.cn

§Corresponding author: xinluphy@zju.edu.cn

is also observed in the superconducting state, similar to the case of $Cu_xBi_2Se_3$ as topological superconductor candidates [12, 13, 14, 15, 16, 11, 17, 18].

So far, various methods such as doping, proximity effect, hydraulic pressure, tip-contact have been applied on nontrivial topological materials in order to induce topological superconductivity and Majorana fermions [10, 6, 7, 8, 19, 20, 21]. Majorana fermions are proposed to play a crucial role in the fault-tolerant quantum computation [22, 23, 24]. Among them, Bi_2Se_3 has served as a characteristic compound of topological insulators susceptible to tuning and emergence of superconductivity [10, 6, 19] and its van der Waals (vdW) structure also implies a potential application in quantum electronic devices, especially when superconductivity can be achieved [25, 26, 27]. However, an easy and controllable condition to realize SC in Bi_2Se_3 is still lacking and thus desirable.

In this paper, an unambiguous superconductivity is observed for the mesoscopic point-contacts on topological insulator Bi_2Se_3 after applying a voltage pulse, evidenced by the Andreev reflection peak in point-contact spectra (PCS) and a resistance drop for the exfoliated Bi_2Se_3 flake samples. Superconductivity emerges only in the case of Ag-Bi_2Se_3 contacts with either silver paints in soft-PCS(SPCS) or Ag tips in mechanical-PCS(MPCS) right after the voltage pulse, but is absent for the Au, Cu or Ti tips, favoring the scenario that the emergent SC is probably due to Ag dopants into the vdW gap of Bi_2Se_3 across the interface. The SC becomes unstable against thermal cycles and disappears when the sample is warmed up to high temperatures, however, it can be re-induced by a new voltage pulse after cooled back to 1.9 K. Our observations strongly support the erasable nature of the SC in the local contact region, ensuring potential applications in quantum devices.

The Bi_2Se_3 crystal is composed of alternating Se-Bi-Se-Bi-Se quintuple layers as shown in Fig. 1a and there exists a weak vdW gap between adjacent quintuple layers, making this material easy to be exfoliated as other vdW materials. Temperature dependent resistivity of Bi_2Se_3 with a sample size of 1073 μm $\times$ 591 μm $\times$ 6.3 μm is shown in Fig. 1b, which has a slight upturn due to its insulating band gap but saturates below 40 K with its gapless surface state, consistent with previous reports [28, 29]. Soft point-contacts are formed by silver paints on Bi_2Se_3 as in Fig. 1c, same as the soft-PCS configuration on $Cu_xBi_2Se_3$ [30]. Fig. 1d shows the soft-PCS conductance curve on Bi_2Se_3 at 1.9 K and only an asymmetric background is observed in the absence of any special features. Interestingly, when a voltage pulse between 4 -10 V with a pulse duration less than 10 ms is applied across the contacts, a reproducible zero-bias conductance peak (ZBCP) can be observed with dips at high bias voltages as in Fig. 1e. Fig. 1f shows the evolution of conductance curves in magnetic field and the ZBCP is gradually suppressed without any peak splitting and finally disappears around 3.0 T. Moreover, the ZBCP gets weaker in intensity with increased temperatures untill around 4.5 K, unambiguously signaling the Andreev reflections

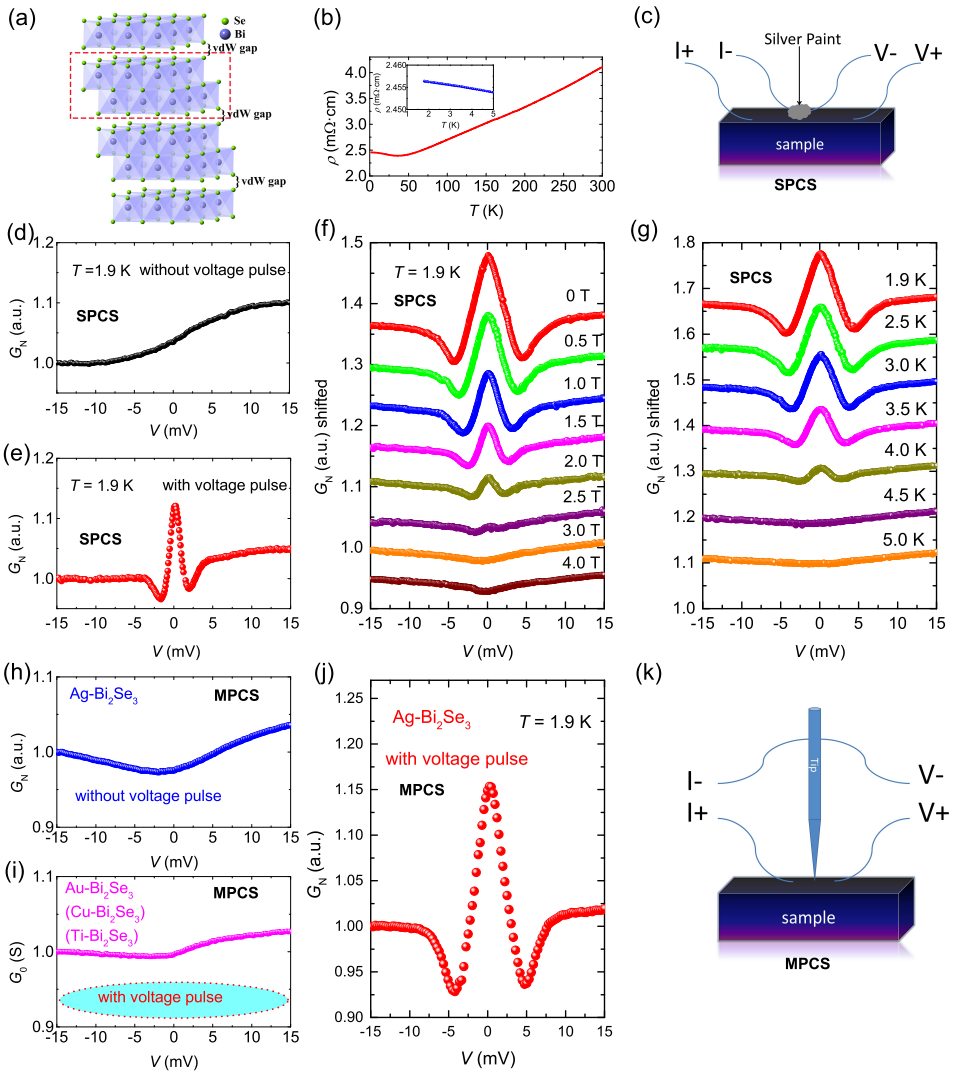

Figure 1: **Evidence for induced superconductivity in mesoscopic Ag point-contact on Bi_2Se_3.** **(a)** The crystal structure of topological insulator Bi_2Se_3 with vdW gap between adjacent Se-Bi-Se-Bi-Se quintuple layers. **(b)** Temperature dependence of the electrical resistivity for the pristine Bi_2Se_3 sample with a dimension of 1073 μm × 591 μm × 6.3 μm. **(c)** Schematic illustration of the soft-PCS electrode configuration on Bi_2Se_3. **(d)** A representative soft-PCS conductance curve for silver paint on the Bi_2Se_3 crystal at 1.9 K without any voltage pulse. G_N is the normalized conductance divided by the conductance value at high voltages. **(e)** A reproducible ZBCP feature in the soft-PCS at 1.9 K after voltage pulse on the contact. **(f)** & **(g)** Magnetic field and temperature evolution of the soft-PCS conductance curves with induced superconductivity in the contact region, respectively. **(h)** & **(i)** Mechanical-PCS conductance curve at 1.9 K for Ag tip before voltage pulse and for Au, Cu or Ti tip after voltage pulse, respectively. **(j)** Mechanical-PCS conductance curve at 1.9 K for Ag tip with induced SC after voltage pulse. **(k)** Schematic illustration of the needle-anvil configuration of mechanical point-contacts.

and induced superconductivity in the contact area by voltage pulses [31, 20, 21]. The maximum superconducting transition temperature T_c for all contacts can be as high as 4.5 K as illustrated by the temperature dependent conductance curves on Bi_2Se_3 in Fig. 1g (or the temperature dependent zero-bias conductance (ZBC) in Fig. S1). We note here that the ZBCP only appears on the contact affected by the voltage pulse and other contacts without it on the same sample would not show any SC trace (Several soft point-contacts on the same sample can be realized in practice).

In comparison with our soft-PCS results, a needle-anvil type of mechanical-PCS was also applied as schematically illustrated in Fig. 1k with several tip options available such as silver, gold, copper or titanium. Similar behaviours are observed for the Ag tip on Bi_2Se_3 crystals after a voltage pulse, where a local SC in the contact can be induced with a characteristic SC ZBCP at 1.9 K. In sharp contrast, Au, Cu or Ti tips on Bi_2Se_3 fail to induce any SC within the maximum voltage pulse $\sim$ 10 V as in Fig. 1i. We would thus speculate that the induced SC in the point-contact area is intimately associated with Ag atoms as a result of voltage pulses.

In order to confirm the probable superconductivity with electrical resistive measurements, the Bi_2Se_3 sample was exfoliated by tape to a very tiny flake and it was transferred onto the pre-deposited Ag electrodes on the silicon substrate as shown in the inset of Fig. 2a, where the space between the neighboring electrode ends is about 3 μm in distance. The temperature dependent electrical resistance for the pristine device is shown in Fig. 2a, which also has an upturn at low temperatures as in Fig. 1b for the bulk sample. Once voltage pulse is applied on the Ag electrodes, a small drop of resistance shows up below 4.5 K ($\sim 1-2\%$) as in Fig. 2a, implying an induced SC as in the PCS measurements. However, the resistance does not go to zero and it is natural to assume a local SC is induced only in the contact region for the Bi_2Se_3 sample. In Fig. 2b, the T_c decreases with increased magnetic field, and the SC transition is totally gone above 2.5 T.

It is interesting to study the stability of this local superconductivity against thermal cycles and the sample resistance over several thermal cycles with a cooling (warming) speed of 3 K/min is shown in Fig. 2c. For the first cycle, the sample is only warmed up to 50 K and then cooled back to 1.9 K, where the SC transition temperature T_c nearly maintains the same value of 4.5 K with the resistance curves overlapping on each other. However, as long as the sample is warmed up to a higher terminal temperature, T_c is gradually reduced and the transition finally disappears after warming up to 300 K. Moreover, superconductivity would emerge once again at 1.9 K after a new voltage pulse on Bi_2Se_3. Meanwhile, our soft-PCS with silver paint shows a consistent behaviour: the ZBCP would disappear in the conductance curves while the zero-bias conductance as a function of temperature shows the absence of any SC transition after thermal cycles as in Fig. 2d. It is thus a strong evidence for the metastable nature of induced SC in the

mesoscopic Ag point-contacts on Bi_2Se_3, which can be repetitively erased by thermal activations.

As for the underlying mechanism of the induced superconductivity in the Ag-Bi_2Se_3 type point-contacts, the voltage pulse can usually generate a considerable local electric field and inject the metallic atoms from the tip to Bi_2Se_3 [32]. The injected Ag atoms should probably be trapped by and intercalated into the vdW gap of Bi_2Se_3 at low temperatures, forming some kind of $Ag_xBi_2Se_3$ with superconductivity in the local region similar to the SC compound $Cu_xBi_2Se_3$. We notice that SC in $Ag_xBi_2Se_3$ has been theoretically proposed via the dynamic mean-field theory with a local density approximation and its T_c is estimated around 4.5 K, pretty similar to our experimental results [33]. It is actually a common practice for atoms to be deposited on substrates in scanning probe microscopic lithography with the help of a voltage pulse on metallic tip [34, 35, 36]. In general, the atomic emission process is strongly dependent on the evaporation field for different atoms, where Ag has a relatively lower evaporation field in comparison with Cu and Au [32, 37, 38]. On the other hand, even though Ti has a much lower evaporation field than Ag, the intercalation of Ti in Bi_2Se_3 probably would not induce SC as in $Ag_xBi_2Se_3$ [33]. Of course, the real atomic emission process can be more complicated and more detailed studies are further needed [32, 39].

The disappearance of superconductivity in the Ag-Bi_2Se_3 mesoscopic point-contacts over thermal cycles probably originates from the instability of Ag intercalation in the Bi_2Se_3 vdW gaps at high temperatures. Considering the weak vdW gap between the Bi_2Se_3 quintuple layers, it is not surprising that no $Ag_xBi_2Se_3$ compound has been reported to be synthesized at room temperatures so far. At 300 K, the intercalated Ag atoms would have escaped from the vdW gap thanks to the thermal activation energy. In comparison, even though SC in $Cu_xBi_2Se_3$ crystals has been widely reported, its superconducting volume fraction shows a high dependence on quench conditions, where quenching from a lower temperature or not quenching at all can be detrimental to SC, strongly supporting the metastable nature of Cu intercalation [40]. A metastable superconductivity by thermal cycles has also been reported in $IrTe_2$ with charge-density-wave (CDW) order as its ground state. For $IrTe_2$, a thermal quench process achieved by current pulses can induce or erase the SC in a tiny exfoliated sample, and it is a kinetic and nonequilibrium approach to induce SC as a metastable state competing with the CDW order [41, 42]. In our case of Bi_2Se_3, the voltage pulse on point-contact can locally heat it to high temperatures and then rapidly cool down, mimicking the thermal quench process. However, the absence of SC in Au, Cu and Ti point-contacts on Bi_2Se_3 argues against the same SC mechanism as in $IrTe_2$, but favors the importance of Ag intercalation.

The erasable SC in mesoscopic point-contacts on Bi_2Se_3 with thermal cycles implies a promising application on logic and memory circuits as an electrical switch, if equipped with a local heater on the contact [43, 44, 45, 46]. A voltage pulse can momentarily drive the sample into

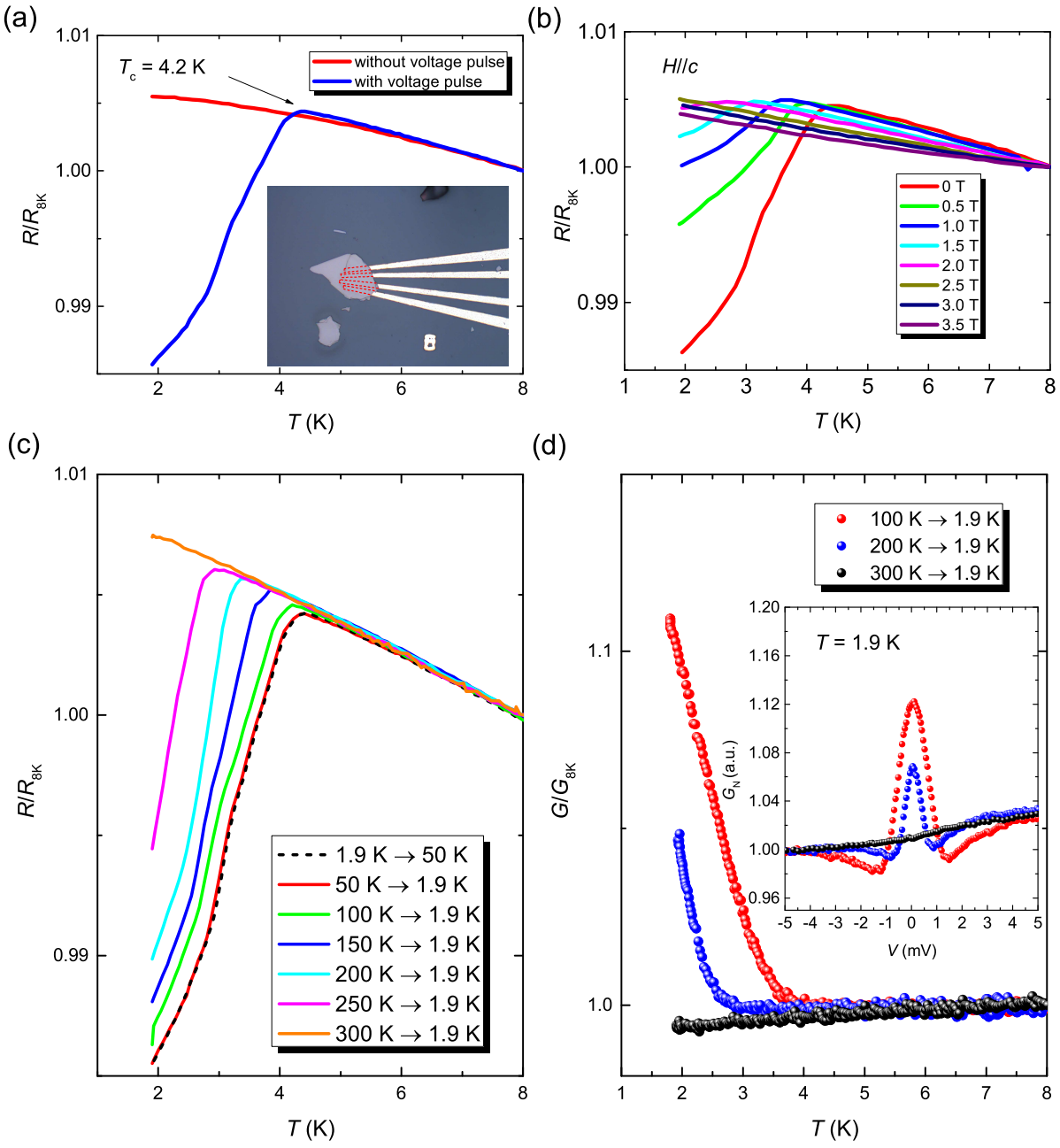

Figure 2: **Evidence of local and erasable superconductivity in Ag-Bi_2Se_3 contacts.** **(a)** Temperature dependence of the electrical resistance for an exfoliated Bi_2Se_3 flake before and after voltage pulse for comparison. The inset is the photo of an exfoliated flake with Ag electrodes pre-deposited on the bottom with the electrode distance ~ 3 μm. **(b)** The evolution of R-T curves in different magnetic fields for the exfoliated Bi_2Se_3 sample after voltage pulse. **(c) & (d)** Temperature dependence of the electrical resistance for exfoliated Bi_2Se_3, and ZBC for silver paint point-contacts after different thermal cycles with a temperature ramping speed of 3 K/min. The inset of (d) shows the Ag-Bi_2Se_3 point-contact conductance at 1.9 K after different thermal cycles.

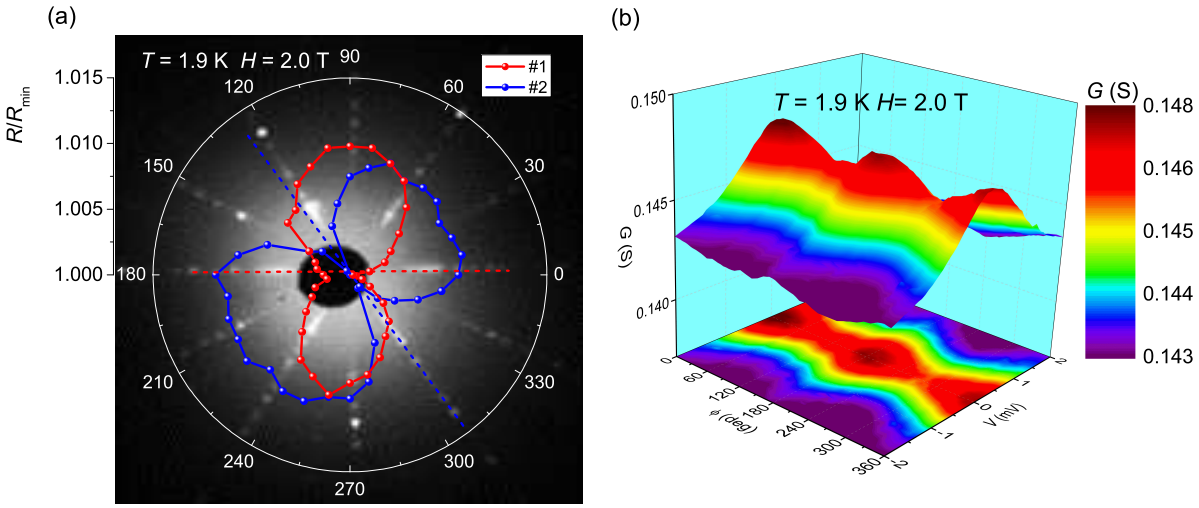

Figure 3: **Field-angle dependence of the soft-PCS of Ag-Bi_2Se_3 with the induced superconductivity. (a)** Field-angle dependence of the ZBR for two contacts #1 and #2 on the same Bi_2Se_3 crystal at 1.9 K with an in-plane field of 2.0 T. The red (blue) dashed line marks the short C_2 axis for its nematic domain #1 (#2), respectively. **(b)** Three-dimensional contour plot of the soft-PCS conductance curves as a function of field angle at 1.9 K and 2.0 T.

superconducting state as a low-resistance phase, while an electrical heater can switch it back to the normal state as a high-resistance phase. This can serve as a phase-change memory while its different resistance states represent 1s and 0s for the stored digital data. The local and erasable superconductivity induced with Ag tip signifies a more accurate and controllable writing/design of superconducting circuits (even topological superconducting circuits) at low temperatures, if scanning probe microscopic lithography method can be introduced [36, 47]. We notice a recent work carried out by the conductive-AFM method on two-dimensional electron gas and our results would facilitate such efforts [48, 49].

Finally, we would like to investigate the superconducting nature of the Ag-doped topological insulator Bi_2Se_3 in our mesoscopic point-contacts, where our field-rotational PCS characterizes a rotational C_4 symmetry breaking and suggests an exotic topological SC as in $Cu_xBi_2Se_3$ [12, 13, 14, 15, 11, 17, 18]. The azimuthal field-angle dependence of the zero-bias point-contact resistance (ZBR) on Bi_2Se_3 after voltage pulse at 1.9 K and in field of 2.0 T is shown in Fig. 3a, where the magnetic field is rotated in the *ab*-plane. A clear 2-fold symmetry of the ZBR is present at 2.0 T, probably signaling a C_2 symmetry of the superconductor gap and thus a nematic SC despite of its hexagonal lattice structure. This 2-fold symmetry is only observed in the superconducting state below its upper critical field $H_{c2} \sim 3.0$ T but absent in the normal state as shown in Fig. S2(a). When fixing the field at 2.0 T, the nematic behaviour disappears exactly around its local T_c as in Fig. S2(b) and Fig. S2(c). In our PCS configuration, the junction current is always along the *c*-axis and perpendicular to the rotational field, so that the

influence of vortex motion and Lorentz effect can be excluded. In Fig. 3a, the azimuthal field-angle dependence of ZBR for two different point-contacts #1 and #2 on the same sample both shows an obvious dumbbell shape but with different long C_2 axis, which are perpendicular to the crystal axis and imply the existence of nematic SC domains in Bi_2Se_3 below T_c. It is a strong evidence to exclude other artificial effects as the two-fold origins, such as sample misalignment, sample geometry or point-contact geometry. The existence of different nematic domains is probably caused by the local strain effect and its microscopic mechanism needs further careful studies.

Field-angle dependence of PCS conductance curves at 1.9 K and 2.0 T is shown in Fig. 3b as a three-dimensional contour plot, where a clear 2-fold symmetry can also be observed from both the peak intensity and width of Andreev reflection signals. The anisotropic magnitude of the nematic behaviour can be roughly estimated by the ratio of maximum/minimum conductance peak width with $1.5/1 \sim 1.5$, which is the result of anisotropic upper critical field H_{c2} in the ab-plane. In the Ginzburg-Landau theory, the H_{c2} is inversely proportional to the square-root product of coherence length ξ in two separate directions orthogonal to the field. We can infer that the maximum of coherence length as well as the SC gap minimum in the ab-plane should be along the crystal axis. Such superconductivity is consistent with a fully gapped Δ_{4y} state in an odd-parity E_u symmetry, implying a topological superconductor in the D_{3d} crystal point group [12, 18]. A similar ZBCP in the PCS on $Cu_xBi_2Se_3$ has been claimed due to Majorana fermions [12, 30], however, we note it can also arise from thermal effect for point-contacts in thermal regimes [31, 50]. Further studies are required to explore the nature and origin of ZBCP for the induced SC in our Ag-Bi_2Se_3 point-contacts.

In conclusion, we have discovered the unexpected superconductivity only in the Ag-Bi_2Se_3 mesoscopic point-contacts by applying a voltage pulse, either in soft- or mechanical- PCS setup, which is rather absent in the case of Au, Cu or Ti contacts within the voltage limit. We propose that the voltage pulse and thus electrical field should inject Ag atoms into the vdW gap of Bi_2Se_3 and induce a local superconductivity. The superconductivity can be erased by thermal cycles, where warming samples up to high temperatures seems to lose the trapped Ag atoms from the weak vdW gap. Our discovery of the erasable and repetitive superconductivity in topological insulator Bi_2Se_3 may pave a new route for applications of quantum electronic devices that harness the power of topological superconductivity and Majorana fermions.

Methods

Resistivity measurement. Electrical resistivity of Bi_2Se_3 was measured by the conventional four-probe method. Electrodes on bulk sample of a larger size were made with silver paint (SPI05001-AB), which can be dry within several minutes, while those on the exfoliated Bi_2Se_3 flake were made with pre-sputtered Ag electrodes on Si/SiO_2 chip and the Bi_2Se_3 flake

was mechanically transferred on the top of Ag electrodes.

Point-contact spectroscopy measurements. Soft point-contacts on Bi_2Se_3 were prepared by attaching a 20 μm diam. gold wire with a silver-paint drop at the end on the freshly-cleaved surface at room temperature. In such a configuration, thousands of parallel nanoscale channels were assumed between individual silver particles and the crystal surface. Mechanical point-contacts on Bi_2Se_3 in a needle-anvil style were prepared by engaging a sharp tip on the sample surface by piezo-controlled nano-positioners. The tips can be Ag, Au, Cu and Ti wires, with sharp apex cut by razor blade. The conductance curves as a function of bias voltage, $G(V)$, were recorded with the conventional lock-in technique in a quasi-four-probe configuration. The output current is mixed with dc and ac components, which were supplied by the model 6221 Keithley current source and model 7265 DSP lock-in amplifier, respectively. The first harmonic response of the lock-in amplifier is proportional to its point-contact resistance $\mathrm{d}V/\mathrm{d}I$ as a function of the biased-voltage V.

Low temperature measurements. Resistivity and point-contact spectroscopy down to 1.9 K were measured in a Quantum Design Physical Property Measurement System (14T-PPMS) equipped with a sample rotator.

Data availability

The authors declare that all relevant data supporting the findings of this study are available within the paper and its Supplementary Information files.

Acknowledgements We are grateful for valuable discussions with Z.A. Xu, H.Q. Yuan, C. Cao and Y. Liu. Work at Zhejiang University was supported by the National Key Research & Development Program of China (Grant No. 2016YFA0300402, No. 2017YFA0303101 and No. 2018YFC0810200) and the National Natural Science Foundation of China (Grant No. 11674279, No. 11374257 and No. 21703204). X.L. would like to acknowledge support from the Zhejiang Provincial Natural Science Foundation of China (LR18A04001). X.W. would like to acknowledge support from Key Research and Development Project of Zhejiang (No. 2018C01048), Zhejiang Lab (No.2018EB0ZX01). We also thank Prmat (Shanghai) Technology Co., Ltd. for their offered Bi_2Se_3 single crystals.

Author contributions The project was conceived by Tian Le, Xiaozhi Wang and Xin Lu; Bi_2Se_3 device on Ag electrodes was designed by Qikai Ye and Xiaozhi Wang. Laue diffraction, resistivity and point-contact spectroscopy measurements were performed by Tian Le and analyzed by Tian Le, Chufan Chen, Lichang Yin, Dongting Zhang, and Xin Lu; Tian Le and Xin Lu wrote the manuscript with input from all authors.

Competing financial interests The authors declare that they have no conflict of interest.

References

[1] M. Z. Hasan, C. L. Kane, Colloquium: Topological insulators, Rev. Mod. Phys. 82 (2010) 3045–3067. doi:10.1103/RevModPhys.82.3045.

[2] X.-L. Qi, S.-C. Zhang, Topological insulators and superconductors, Rev. Mod. Phys. 83 (2011) 1057–1110. doi:10.1103/RevModPhys.83.1057.

[3] H. Zhang, C. X. Liu, X. L. Qi, X. Dai, Z. Fang, S.-C. Zhang, Topological insulators in Bi_2Se_3, Bi_2Te_3 and Sb_2Te_3 with a single Dirac cone on the surface, Nature Phys. 5 (6) (2009) 438. doi:10.1038/nphys1270.

[4] Y. Xia, D. Qian, D. Hsieh, L. Wray, A. Pal, H. Lin, A. Bansil, D. Grauer, Y. S. Hor, R. J. Cava, et al., Observation of a large-gap topological-insulator class with a single dirac cone on the surface, Nature Phys. 5 (6) (2009) 398. doi:10.1038/nphys1274.

[5] L. Fu, C. L. Kane, Superconducting proximity effect and majorana fermions at the surface of a topological insulator, Phys. Rev. Lett. 100 (2008) 096407. doi:10.1103/PhysRevLett.100.096407.

[6] M. X. Wang, C. Liu, J. P. Xu, F. Yang, L. Miao, M. Y. Yao, C. L. Gao, C. Shen, X. Ma, X. Chen, et al., The coexistence of superconductivity and topological order in the Bi_2Se_3 thin films, Science 336 (6077) (2012) 52–55. doi:10.1126/science.1216466.

[7] M. Veldhorst, M. Snelder, M. Hoek, T. Gang, V. K. Guduru, X. L. Wang, U. Zeitler, W. G. van der Wiel, A. A. Golubov, H. Hilgenkamp, et al., Josephson supercurrent through a topological insulator surface state, Nature Mater. 11 (5) (2012) 417. doi:10.1038/nmat3255.

[8] E. Wang, H. Ding, A. V. Fedorov, W. Yao, Z. Li, Y.-F. Lv, K. Zhao, L.-G. Zhang, Z. Xu, J. Schneeloch, et al., Fully gapped topological surface states in Bi_2Se_3 films induced by a d-wave high-temperature superconductor, Nature Phys. 9 (10) (2013) 621. doi:10.1038/nphys2744.

[9] H.-H. Sun, K.-W. Zhang, L.-H. Hu, C. Li, G.-Y. Wang, H.-Y. Ma, Z.-A. Xu, C.-L. Gao, D.-D. Guan, Y.-Y. Li, C. Liu, D. Qian, Y. Zhou, L. Fu, S.-C. Li, F.-C. Zhang, J.-F. Jia, Majorana zero mode detected with spin selective Andreev reflection in the vortex of a topological superconductor, Phys. Rev. Lett. 116 (2016) 257003. doi:10.1103/PhysRevLett.116.257003.

[10] Y. S. Hor, A. J. Williams, J. G. Checkelsky, P. Roushan, J. Seo, Q. Xu, H. W. Zandbergen, A. Yazdani, N. P. Ong, R. J. Cava, Superconductivity in $Cu_xBi_2Se_3$ and its implications

for pairing in the undoped topological insulator, Phys. Rev. Lett. 104 (2010) 057001. doi:10.1103/PhysRevLett.104.057001.

[11] R. Tao, Y.-J. Yan, X. Liu, Z.-W. Wang, Y. Ando, Q.-H. Wang, T. Zhang, D.-L. Feng, Direct visualization of the nematic superconductivity in $Cu_xBi_2Se_3$, Phys. Rev. X 8 (2018) 041024. doi:10.1103/PhysRevX.8.041024.

[12] L. Fu, Odd-parity topological superconductor with nematic order: Application to $Cu_xBi_2Se_3$, Phys. Rev. B 90 (2014) 100509. doi:10.1103/PhysRevB.90.100509.

[13] K. Matano, M. Kriener, K. Segawa, Y. Ando, G. Q. Zheng, Spin-rotation symmetry breaking in the superconducting state of $Cu_xBi_2Se_3$, Nat. Phys. 12 (2016) 852–854. doi:10.1038/nphys3907.

[14] S. Yonezawa, K. Tajiri, S. Nakata, Y. Nagai, Z. Wang, K. Segawa, Y. Ando, Y. Maenos, Thermodynamic evidence for nematic superconductivity in $Cu_xBi_2Se_3$, Nat. Phys. 13 (2017) 123–126. doi:10.1038/nphys3907.

[15] T. Asaba, B. J. Lawson, C. Tinsman, L. Chen, P. Corbae, G. Li, Y. Qiu, Y. S. Hor, L. Fu, L. Li, Rotational symmetry breaking in a trigonal superconductor Nb-doped Bi_2Se_3, Phys. Rev. X 7 (2017) 011009. doi:10.1103/PhysRevX.7.011009.

[16] X. Chen, M.and Chen, H. Yang, Z. Du, H. H. Wen, Superconductivity with twofold symmetry in $Bi_2Se_3/FeTe_{0.55}Se_{0.45}$ heterostructures, Sci. Adv. 4 (2018) eaat1084. doi:10.1126/sciadv.aat1084.

[17] Y. Sun, S. Kittaka, T. Sakakibara, K. Machida, J. Wang, J. Wen, X. Xing, Z. Shi, T. Tamegai, Quasiparticle evidence for the nematic state above $Sr_xBi_2Se_3$, Phys. Rev. Lett. 123 (2019) 027002. doi:10.1103/PhysRevLett.123.027002.

[18] J. W. F. Venderbos, V. Kozii, L. Fu, Odd-parity superconductors with two-component order parameters: Nematic and chiral, full gap, and majorana node, Phys. Rev. B 94 (2016) 180504. doi:10.1103/PhysRevB.94.180504.

[19] K. Kirshenbaum, P. S. Syers, A. P. Hope, N. P. Butch, J. R. Jeffries, S. T. Weir, J. J. Hamlin, M. B. Maple, Y. K. Vohra, J. Paglione, Pressure-induced unconventional superconducting phase in the topological insulator Bi_2Se_3, Phys. Rev. Lett. 111 (2013) 087001. doi:10.1103/PhysRevLett.111.087001.

[20] L. Aggarwal, A. Gaurav, G. S. Thakur, Z. Haque, A. K. Ganguli, G. Sheet, Unconventional superconductivity at mesoscopic point contacts on the 3D Dirac semimetal Cd_3As_2, Nature Mater. 15 (1) (2016) 32. doi:10.1038/nmat4455.

[21] H. Wang, H. Wang, H. Liu, H. Lu, W. Yang, S. Jia, X.-J. Liu, X. Xie, J. Wei, J. Wang, Observation of superconductivity induced by a point contact on 3D Dirac semimetal Cd_3As_2 crystals, Nature Mater. 15 (1) (2016) 38. doi:10.1038/nmat4456.

[22] C. Nayak, S. H. Simon, A. Stern, M. Freedman, S. Das Sarma, Non-Abelian anyons and topological quantum computation, Rev. Mod. Phys. 80 (2008) 1083–1159. doi:10.1103/RevModPhys.80.1083.

[23] J. Alicea, Y. Oreg, G. Refael, F. Von Oppen, M. P. Fisher, Non-Abelian statistics and topological quantum information processing in 1D wire networks, Nature Phys. 7 (5) (2011) 412. doi:10.1038/nphys1915.

[24] R. M. Lutchyn, J. D. Sau, S. Das Sarma, Majorana fermions and a topological phase transition in semiconductor-superconductor heterostructures, Phys. Rev. Lett. 105 (2010) 077001. doi:10.1103/PhysRevLett.105.077001.

[25] A. K. Geim, I. V. Grigorieva, Van der Waals heterostructures, Nature 499 (7459) (2013) 419. doi:10.1038/nature12385.

[26] Y. Liu, Y. Huang, X. Duan, Van der Waals integration before and beyond two-dimensional materials, Nature 567 (7748) (2019) 323. doi:10.1038/s41586-019-1013-x.

[27] D. Basov, M. Fogler, F. G. De Abajo, Polaritons in van der Waals materials, Science 354 (6309) (2016) aag1992. doi:10.1126/science.aag1992.

[28] N. P. Butch, K. Kirshenbaum, P. Syers, A. B. Sushkov, G. S. Jenkins, H. D. Drew, J. Paglione, Strong surface scattering in ultrahigh-mobility Bi_2Se_3 topological insulator crystals, Phys. Rev. B 81 (2010) 241301. doi:10.1103/PhysRevB.81.241301.

[29] D. Kim, Q. Li, P. Syers, N. P. Butch, J. Paglione, S. D. Sarma, M. S. Fuhrer, Intrinsic electron-phonon resistivity of Bi_2Se_3 in the topological regime, Phys. Rev. Lett. 109 (2012) 166801.

[30] S. Sasaki, M. Kriener, K. Segawa, K. Yada, Y. Tanaka, M. Sato, Y. Ando, Topological superconductivity in $Cu_xBi_2Se_3$, Phys. Rev. Lett. 107 (2011) 217001. doi:10.1103/PhysRevLett.107.217001.

[31] G. Sheet, S. Mukhopadhyay, P. Raychaudhuri, Role of critical current on the point-contact Andreev reflection spectra between a normal metal and a superconductor, Phys. Rev. B 69 (2004) 134507. doi:10.1103/PhysRevB.69.134507.

[32] T. T. Tsong, Effects of an electric field in atomic manipulations, Phys. Rev. B 44 (1991) 13703–13710. doi:10.1103/PhysRevB.44.13703.

[33] S. Koley, S. Basu, Superconductivity induced by Ag intercalation in Dirac semimetal Bi_2Se_3, arXiv:1904.03698 (2019).

[34] H. J. Mamin, P. H. Guethner, D. Rugar, Atomic emission from a gold scanning-tunneling-microscope tip, Phys. Rev. Lett. 65 (1990) 2418–2421. doi:10.1103/PhysRevLett.65.2418.

[35] H. M. Saavedra, T. J. Mullen, P. Zhang, D. C. Dewey, S. A. Claridge, P. S. Weiss, Hybrid strategies in nanolithography, Rep. Prog. Phys. 73 (3) (2010) 036501. doi:10.1088/0034-4885/73/3/036501.

[36] R. Garcia, A. W. Knoll, E. Riedo, Advanced scanning probe lithography, Nat. Nano. 9 (8) (2014) 577. doi:10.1038/nnano.2014.157.

[37] T. Tsong, Field ion image formation, Surface Science 70 (1) (1978) 211–233. doi:10.1016/0039-6028(78)90410-7.

[38] S. Katano, M. Hotsuki, Y. Uehara, Creation and luminescence of a single silver nanoparticle on Si (111) investigated by scanning tunneling microscopy, J. Phys. Chem. C 120 (50) (2016) 28575–28582. doi:10.1063/1.5011002.

[39] M. Olsen, M. Hummelgård, H. Olin, Surface modifications by field induced diffusion, PLoS One 7 (1) (2012) e30106. doi:10.1371/journal.pone.0030106.

[40] J. A. Schneeloch, R. D. Zhong, Z. J. Xu, G. D. Gu, J. M. Tranquada, Dependence of superconductivity in $Cu_xBi_2Se_3$ on quenching conditions, Phys. Rev. B 91 (2015) 144506. doi:10.1103/PhysRevB.91.144506.

[41] H. Oike, M. Kamitani, Y. Tokura, F. Kagawa, Kinetic approach to superconductivity hidden behind a competing order, Sci. Adv. 4 (10) (2018) eaau3489. doi:10.1126/sciadv.aau3489.

[42] M. Yoshida, K. Kudo, M. Nohara, Y. Iwasa, Metastable superconductivity in two-dimensional $IrTe_2$ crystals, Nano lett. 18 (5) (2018) 3113–3117. doi:10.1021/acs.nanolett.8b00673.

[43] G. Meijer, Who wins the nonvolatile memory race?, Science 319 (5870) (2008) 1625–1626. doi:10.1126/science.1153909.

[44] D. B. Strukov, G. S. Snider, D. R. Stewart, R. S. Williams, The missing memristor found, Nature 453 (7191) (2008) 80. doi:10.1038/nature06932.

[45] D.-H. Kwon, K. M. Kim, J. H. Jang, J. M. Jeon, M. H. Lee, G. H. Kim, X.-S. Li, G.-S. Park, B. Lee, S. Han, et al., Atomic structure of conducting nanofilaments in TiO_2 resistive switching memory, Nat. Nano. 5 (2) (2010) 148. doi:10.1038/nnano.2009.456.

[46] K. Szot, W. Speier, G. Bihlmayer, R. Waser, Switching the electrical resistance of individual dislocations in single-crystalline $SrTiO_3$, Nat. Mater. 5 (4) (2006) 312. doi:10.1038/nmat1614.

[47] A. A. Tseng, A. Notargiacomo, T. Chen, Nanofabrication by scanning probe microscope lithography: A review, J. Vac. Sci. Tech. B 23 (3) (2005) 877–894. doi:10.1116/1.1926293.

[48] Y.-Y. Pai, H. Lee, J.-W. Lee, A. Annadi, G. Cheng, S. Lu, M. Tomczyk, M. Huang, C.-B. Eom, P. Irvin, J. Levy, One-dimensional nature of superconductivity at the $LaAlO_3/SrTiO_3$ interface, Phys. Rev. Lett. 120 (2018) 147001. doi:10.1103/PhysRevLett.120.147001.

[49] C. Cen, S. Thiel, G. Hammerl, C. W. Schneider, K. Andersen, C. Hellberg, J. Mannhart, J. Levy, Nanoscale control of an interfacial metal–insulator transition at room temperature, Nature Mater. 7 (4) (2008) 298–302. doi:10.1038/nmat2136.

[50] D. Dagher, R. S. Gonnelli, Probing multiband superconductivity by point-contact spectroscopy, Supercond. Sci. Technol. 23 (4) (2010) 043001. doi:10.1088/0953-2048/23/4/043001.

Figures

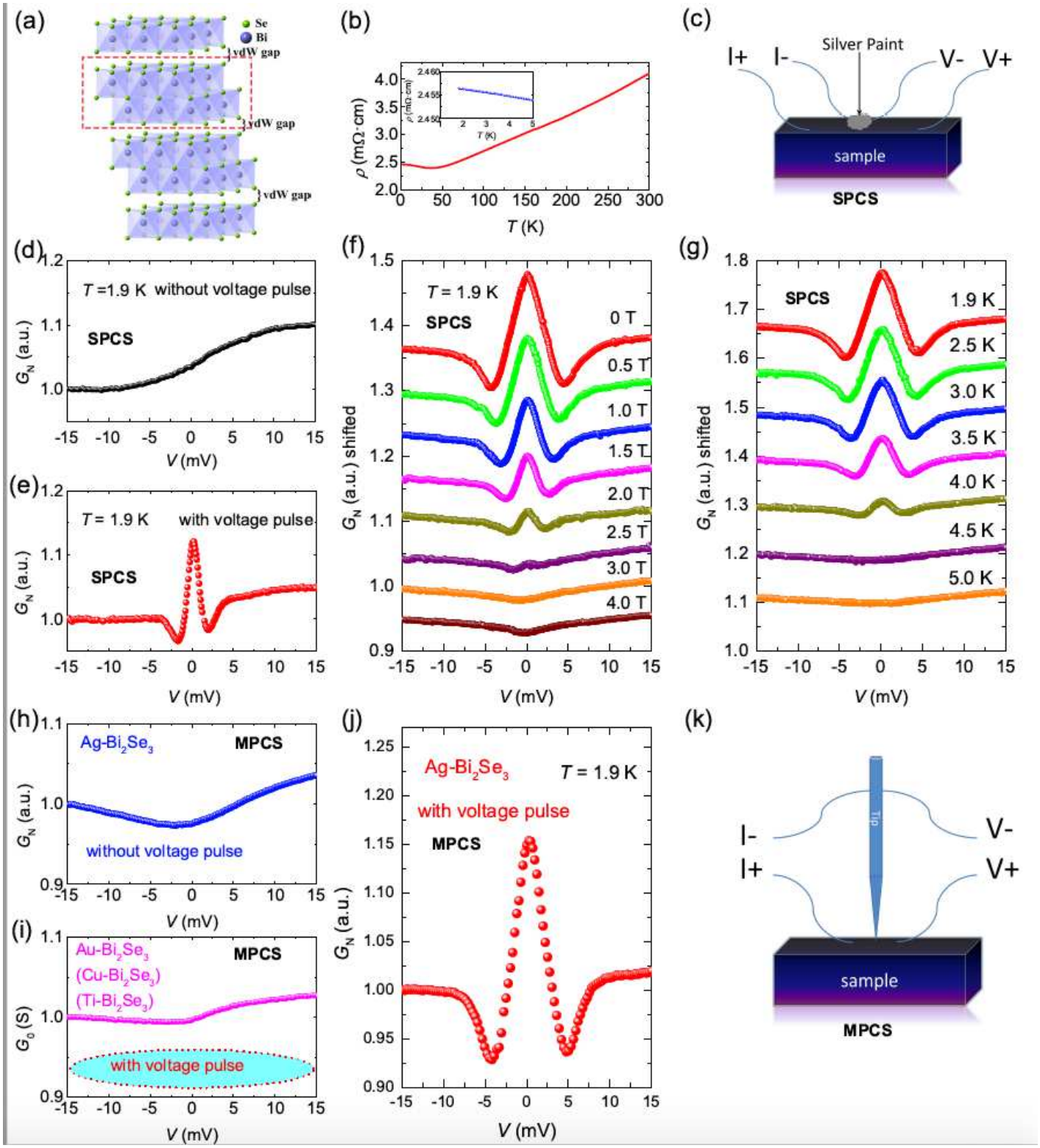

Figure 1

Evidence for induced superconductivity in mesoscopic Ag point-contact on Bi2Se3. (a) The crystal structure of topological insulator Bi2Se3 with vdW gap between adjacent Se-Bi-Se-Bi-Se quintuple layers. (b) Temperature dependence of the electrical resistivity for the pristine Bi2Se3 sample with a dimension

of 1073 μm x 591 μm x 6.3 μm. (c) Schematic illustration of the soft-PCS electrode configuration on Bi2Se3. (d) A representative soft-PCS conductance curve for silver paint on the Bi2Se3 crystal at 1.9 K without any voltage pulse. GN is the normalized conductance divided by the conductance value at high voltages. (e) A reproducible ZBCP feature in the soft-PCS at 1.9 K after voltage pulse on the contact. (f) & (g) Magnetic eld and temperature evolution of the soft-PCS conductance curves with induced superconductivity in the contact region, respectively. (h) & (i) Mechanical-PCS conductance curve at 1.9 K for Ag tip before voltage pulse and for Au, Cu or Ti tip after voltage pulse, respectively. (j) Mechanical-PCS conductance curve at 1.9 K for Ag tip with induced SC after voltage pulse. (k) Schematic illustration of the needle-anvil configuration of mechanical point-contacts.

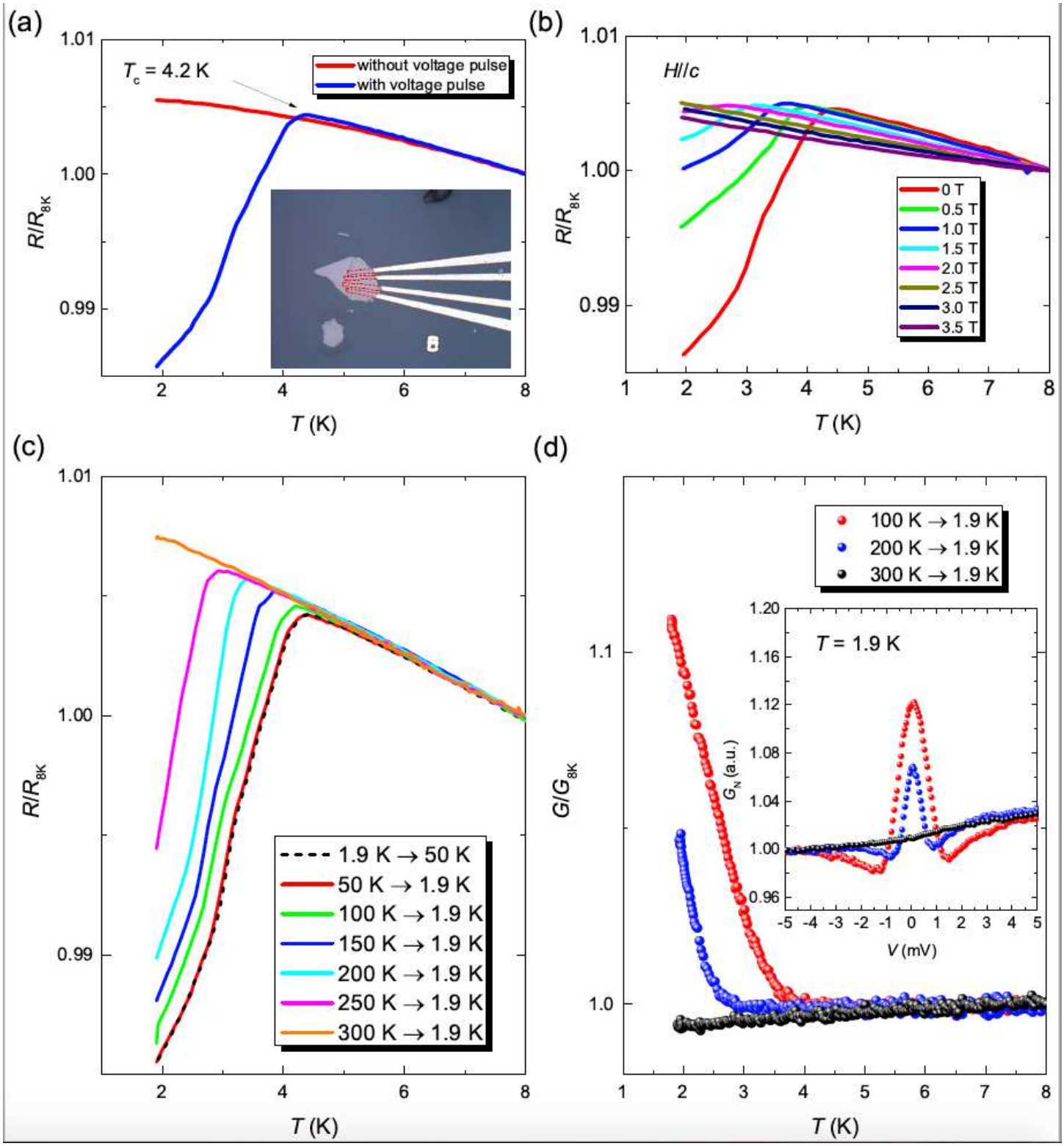

Figure 2

Evidence of local and erasable superconductivity in Ag-Bi2Se3 contacts. (a) Temperature dependence of the electrical resistance for an exfoliated Bi2Se3 flake before and after voltage pulse for comparison. The inset is the photo of an exfoliated flake with Ag electrodes pre-deposited on the bottom with the electrode distance ~ 3 μm. (b) The evolution of R-T curves in different magnetic fields for the exfoliated Bi2Se3 sample after voltage pulse. (c) & (d) Temperature dependence of the electrical resistance for exfoliated

Bi2Se3, and ZBC for silver paint point-contacts after different thermal cycles with a temperature ramping speed of 3 K/min. The inset of (d) shows the Ag-Bi2Se3 point-contact conductance at 1.9 K after different thermal cycles.

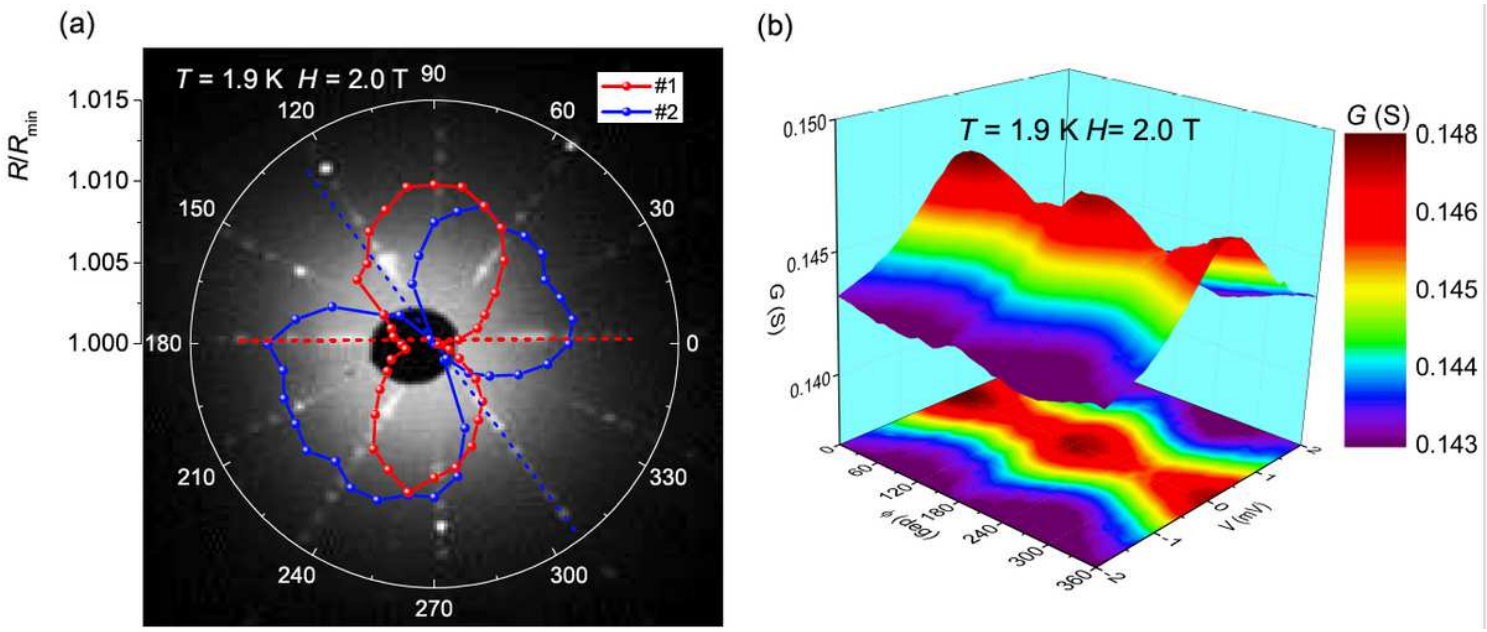

Figure 3

Field-angle dependence of the soft-PCS of Ag-Bi2Se3 with the induced superconductivity. (a) Field-angle dependence of the ZBR for two contacts #1 and #2 on the same Bi2Se3 crystal at 1.9 K with an in-plane eld of 2.0 T. The red (blue) dashed line marks the short C2 axis for its nematic domain #1 (#2), respectively. (b) Three-dimensional contour plot of the soft-PCS conductance curves as a function of eld angle at 1.9 K and 2.0 T.

Supplementary Files

This is a list of supplementary files associated with this preprint. Click to download.

- Supplementary.pdf